

## HEAT AND MASS TRANSPORT ASPECTS OF NANOFLUID FLOW TOWARDS A VERTICAL FLAT SURFACE INFLUENCED BY ELECTRIFIED NANOPARTICLES AND ELECTRIC REYNOLDS NUMBER

Aditya Kumar Pati, Sujit Mishra, Ashok Misra\*, Saroj Kumar Mishra

Centurion University of Technology and Management, Paralakhemundi, Odisha, India

\*Corresponding author e-mail: [amisra1972@gmail.com](mailto:amisra1972@gmail.com)

Received April 6, 2024; revised May 3, 2024; accepted May 15, 2024

This study examines the heat and mass transfer aspects of the natural convective flow of a nanofluid along a vertical flat surface, incorporating electrified nanoparticles and electric Reynolds number. While conventional nanofluid models like Buongiorno's model overlook the nanoparticle electrification and electric Reynolds number mechanisms, this study addresses the nanoparticle electrification and electric Reynolds number mechanisms by justifying its relevance, particularly when tribo-electrification results from Brownian motion. This incorporation of the electric Reynolds number and nanoparticle electrification mechanism is a unique aspect of this investigation. Using the similarity method and nondimensionalization, the governing partial differential equations of the flow are transformed into a set of locally similar equations. MATLAB's `bvp4c` solver is employed to solve this set of equations, along with the boundary conditions. The obtained results are validated by comparison with those from previously published works. Graphical representations are provided for the numerical outcomes of non-dimensional velocity, concentration and temperature concerning the nanoparticle electrification parameter and electric Reynolds number. The combined effects of the nanoparticle electrification parameter and the electric Reynolds number on non-dimensional heat and mass transfer coefficients are examined in tabular form. Furthermore, the impact of the nanoparticle electrification parameter on both heat and mass transfer for varying values of the Brownian motion parameter is explored graphically. The primary finding of this investigation indicates that the electrification mechanism of nanoparticles quickens the transfer of heat and mass from a flat surface to nanofluid, suggesting promising prospects for utilization in cooling systems and biomedical applications.

**Keywords:** *Electrified Nanoparticles; Nanofluid; Buongiorno's model; Electric Reynolds number; Natural convection*

**PACS:** 44.20.+b, 44.25.+f, 47.10.ad, 47.55.pb, 47.15.Cb

### 1. INTRODUCTION

The incorporation of heat and mass transfer in the natural convective boundary layer flow around a vertical flat surface has garnered significant interest due to its myriad practical implications. These include applications in industries such as crude oil extraction, nuclear waste storage, packed bed reactors, aviation insulation, heat exchangers, geothermal ventures, and the cooling of electronic equipment. These examples underscore the utilization of the earth's natural heat across various technological domains. Recent technological advancements in the manipulation of standard fluids now involve the integration of nanometer-sized particle fibers into primary fluids, leading to the creation of nanofluids. These nanofluids are primarily utilized to augment the heat transfer capabilities of the base fluid. Over time, the progression and refinement of technology, particularly in the realm of nanotechnology, are expected to significantly impact future markets. Nanotechnology, which involves the study and application of structures at the nanoscale level, has facilitated the development of various effective products. Its applications span across multiple domains, including medicine, therapy, diagnostics, sequencing, electronics, and material manufacturing. Choi et al. [1] illustrated that adding nanoparticles to a base fluid can significantly enhance thermal conductivity, effectively doubling it.

Several researchers have proposed numerous physical factors that enhance heat transmission in nanofluid flow. Buongiorno [2] emphasized that thermophoresis and Brownian motion are pivotal slip mechanisms for modelling nanofluid flow. However, the impact of nanoparticle electrification and electric Reynolds number mechanisms has been overlooked in this context. Several studies (Kuznetsov and Nield [3], Khan and Aziz [4], Aziz and Khan [5], Das and Jana [6], Goyal and Bhargabha [7], Jeevandar et al. [8], Reddy and Goud [9], Dey et al. [10]) have explored the simulation of free convective nanofluid flow along a vertical flat plate using Buongiorno's model [2]. Notably, the mechanism of nanoparticle electrification remains unaddressed in all these studies ([2] to [10]). Nonetheless, due to Brownian motion leading to nanoparticle collisions, the significance of the electrification mechanism is justified (Soo [11]; Kang and Wang [12]).

This study delves into the combined effects of electric Reynolds number and electrified nanoparticles on the flow of nanofluid near a vertical flat surface. Integrating the electric Reynolds number and electrified nanoparticles into Buongiorno's model allows for an exploration of the heat and mass transport dynamics of the nanofluid, which is a uniqueness of the current work not considered in earlier literature on nanofluid flow past a vertical flat surface.

## 2. MATHEMATICAL FORMULATION

A  $Cu$ -water steady laminar nanofluid flow with electrified nanoparticles is examined. The vertical flat surface is chosen along the  $x$  axis. The wall surface maintains constant values for concentration ( $C_w$ ) and temperature ( $T_w$ ). The values for temperature and concentration outside the boundary layer are taken as  $T_\infty$  and  $C_\infty$ , respectively. The schematic view is displayed in Fig 1.

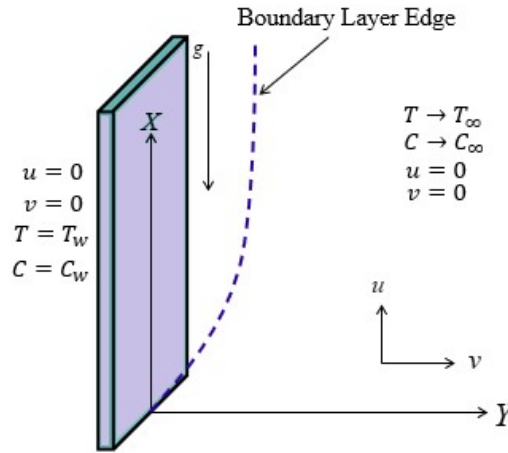


Figure 1. Coordinate system and schematic view

The governing equations with electrified nanoparticles (Pati et al. [13]) and using the Oberbeck-Boussinesq approach can be formulated as follows:

$$\frac{\partial u}{\partial x} + \frac{\partial v}{\partial y} = 0, \quad (1)$$

$$\rho_{nf} \left( u \frac{\partial u}{\partial x} + v \frac{\partial u}{\partial y} \right) = \rho_s \frac{q}{m} (C - C_\infty) E_x + \mu_{nf} \left( \frac{\partial^2 u}{\partial y^2} \right) + (T - T_\infty) \beta_{f\infty} \rho_{f\infty} g (1 - C_\infty) - (\rho_s - \rho_{f\infty}) (C - C_\infty) g, \quad (2)$$

$$u \frac{\partial T}{\partial x} + v \frac{\partial T}{\partial y} = \frac{(\rho c)_s}{(\rho c)_{nf}} \frac{q}{m} \frac{C}{F} \left( E_x \frac{\partial T}{\partial x} + E_y \frac{\partial T}{\partial y} \right) + \frac{k_{nf}}{(\rho c)_{nf}} \left( \frac{\partial^2 T}{\partial y^2} \right) + \frac{(\rho c)_s}{(\rho c)_{nf}} \frac{D_T}{T_\infty} \left( \frac{\partial T}{\partial y} \right)^2 + \frac{(\rho c)_s}{(\rho c)_{nf}} D_B \frac{\partial C}{\partial y} \frac{\partial T}{\partial y} \quad (3)$$

$$u \frac{\partial C}{\partial x} + v \frac{\partial C}{\partial y} = \frac{D_T}{T_\infty} \frac{\partial^2 T}{\partial y^2} + \left( \frac{q}{m} \right) \frac{1}{F} \left[ \frac{\partial(C E_x)}{\partial x} + \frac{\partial(C E_y)}{\partial y} \right] + D_B \frac{\partial^2 C}{\partial y^2}, \quad (4)$$

$$\frac{\partial E_y}{\partial y} = \frac{\rho_s q}{\epsilon_0 m}, \quad (5)$$

and the boundary conditions:

$$\left. \begin{aligned} y = 0, v = 0, u = 0, C = C_w, T = T_w \\ y \rightarrow \infty, v = 0, u = 0, C \rightarrow C_\infty, T \rightarrow T_\infty \end{aligned} \right\} \quad (6)$$

where  $C$  and  $T$  signify the local concentration and local temperature, respectively. The velocity and electric intensity components in the  $(x, y)$  direction is represented by  $(u, v)$  and  $(E_x, E_y)$ , respectively. The subscripts  $f$ ,  $s$  and  $nf$  represent the base fluid, nanoparticle, and nanofluid thermophysical properties, respectively. The symbols  $(\rho c)$ ,  $k$ ,  $\mu$ , and  $\rho$  signify heat capacity, thermal conductivity, viscosity, and density, respectively.  $F$  represents the momentum transfer time constant between the fluid and the nanoparticles.  $g$  denotes the gravitational acceleration.  $D_T$ ,  $\beta_f$  and  $D_B$  stands the thermophoretic diffusion coefficient, volumetric thermal expansion coefficient and Brownian diffusion coefficient, respectively.  $m$  and  $q$  denotes the mass and charge of the nanoparticles, respectively.  $\epsilon_0$  denotes the permittivity. The free stream values are represented by the subscript  $\infty$ .

By considering the stream function  $\psi$  with  $\frac{\partial \psi}{\partial x} = -v$  and  $\frac{\partial \psi}{\partial y} = u$ , equation (1) is clearly satisfied. The variables mentioned below are employed in transforming equations (2), (3), and (4) into equations (8), (9), and (10) and the equations (1) and (5) are identically satisfied.

$$\eta = \frac{y}{x} (Ra_x)^{\frac{1}{4}}, \psi = \alpha_f (Ra_x)^{\frac{1}{4}} f(\eta), s(\eta) = \frac{C - C_\infty}{C_w - C_\infty}, \theta(\eta) = \frac{T - T_\infty}{T_w - T_\infty}, \quad (7)$$

where  $\eta$  denotes similarity variable and  $Ra_x = \frac{x^3 (T_w - T_\infty) \beta_f g (1 - C_\infty)}{\alpha_f \nu_f}$ , is the local Rayleigh number.

The non-dimensional equations are as follows:

$$f'''' + \frac{\phi_1}{4Pr} [3ff'' - 2(f')^2] + \frac{\phi_1\phi_2M}{PrN_F} s + \frac{1}{\phi_5} (\theta - Nr s) = 0, \tag{8}$$

$$\theta'' + \frac{1}{\phi_4} Pr Nt (\theta')^2 + \frac{1}{\phi_4} Sc Nb \left[ \frac{N_F}{N_{Re}} - \frac{1}{4} M \right] (s + Nc) \eta \theta' + \frac{1}{\phi_4} Pr Nbs' \theta' + \frac{3}{4} \frac{1}{\phi_3 \phi_4} f \theta' = 0, \tag{9}$$

$$s'' + \frac{Nt}{Nb} \theta'' - \frac{1}{4} \frac{M Sc}{Pr} \eta s' + \frac{N_F Sc}{Pr N_{Re}} (\eta s' + s + Nc) + \frac{3}{4} \frac{Sc}{Pr} f s' = 0, \tag{10}$$

where prime (') indicates derivative with respect to  $\eta$ .  
 The equations (6) are simplified to

$$\left. \begin{aligned} \eta = 0, f(0) = f'(0) = 0, s(0) = \theta(0) = 1 \\ \eta \rightarrow \infty, f'(\infty) \rightarrow 0, s(\infty) \rightarrow 0, \theta(\infty) \rightarrow 0 \end{aligned} \right\} \tag{11}$$

The nondimensional parameters are represented as

$$\begin{aligned} Nr &= \frac{(\rho_s - \rho_f)(C_w - C_\infty)}{(1 - C_\infty)\rho_f\beta_f(T_w - T_\infty)}, Nt = \frac{(\rho c)_s D_T (T_w - T_\infty)}{(\rho c)_f \nu_f T_\infty}, Pr = \frac{\nu_f}{\alpha_f}, \\ Nc &= \frac{C_\infty}{(C_w - C_\infty)}, Nb = \frac{(\rho c)_s D_B (C_w - C_\infty)}{(\rho c)_f \nu_f}, Sc = \frac{\nu_f}{D_B}, \\ \frac{1}{N_{Re}} &= \left(\frac{q}{m}\right)^2 \frac{\rho_s}{\epsilon_0} \frac{x^2}{\left(\frac{\alpha_f (Ra_x)^{\frac{1}{2}}}{x}\right)^2}, N_F = \frac{\left(\frac{\alpha_f (Ra_x)^{\frac{1}{2}}}{x}\right)}{F_x}, M = \left(\frac{q}{m}\right) \frac{1}{F \left(\frac{\alpha_f (Ra_x)^{\frac{1}{2}}}{x}\right)} E_x. \end{aligned}$$

Here  $Nr$ ,  $Nt$ ,  $Pr$ ,  $Nc$ ,  $Nb$ ,  $Sc$ ,  $N_{Re}$ ,  $N_F$ , and  $M$  denote the buoyancy ratio, thermophoresis parameter, Prandtl number, concentration ratio, Brownian motion parameter, Schmidt number, electric Reynolds number, momentum transfer number, and electrification parameter, respectively.

The thermophysical constants (Maharukh et al., [14]) are represented as

$$\begin{aligned} \phi_1 &= \frac{\nu_f}{\nu_{nf}} = \left[ C_\infty \frac{\rho_s}{\rho_f} + (1 - C_\infty) \right] (1 - C_\infty)^{2.5}, \\ \phi_2 &= \frac{c_f}{c_s} \frac{1}{\left[ \frac{\rho_s C_\infty + (1 - C_\infty)}{\rho_f} \right]}, \tau = \frac{(\rho c)_s}{(\rho c)_f}, \\ \phi_3 &= \frac{(\rho c)_f}{(\rho c)_{nf}} = \frac{1}{C_\infty \tau + (1 - C_\infty)}, \\ \phi_4 &= \frac{k_{nf}}{k_f} = \frac{(k_s + 2k_f) - 2C_\infty(k_f - k_s)}{(k_s + 2k_f) - C_\infty(k_s - k_f)}, \\ \phi_5 &= \frac{\mu_{nf}}{\mu_f} = (1 - C_\infty)^{-2.5}. \end{aligned}$$

The investigation utilizes a nanofluid with a 1% concentration of copper nanoparticles. The thermophysical characteristics of both pure water and the nanoparticles are evaluated based on the criteria established by Oztop and Abu-Nada [15].

The local Nusselt number  $Nu_x$  and Sherwood number  $Sh_x$  are provided for applications involving heat and mass transfer as

$$\begin{aligned} Nu_x &= \frac{xq_w}{k_f(T_w - T_\infty)}, \text{ where } q_w = -k_f \left( \frac{\partial T}{\partial y} \right)_{y=0}, \\ Sh_x &= \frac{xq_m}{D_B(C_w - C_\infty)}, \text{ where } q_m = -D_B \left( \frac{\partial C}{\partial y} \right)_{y=0}. \end{aligned}$$

The reduced Nusselt number  $(-\theta'(0))$  and the reduced Sherwood number  $(-s'(0))$  can be expressed in dimensionless form as

$$\begin{aligned} Nu_x / (Ra_x)^{1/4} &= -\theta'(0), \\ Sh_x / (Ra_x)^{1/4} &= -s'(0). \end{aligned}$$

### 3. METHOD OF SOLUTION

The MATLAB bvp4c solver is employed for solving equations (8) to (10) along with the equation (11) and it is noted that these equations are specifically local similarity equations, as the parameters  $M$ ,  $N_F$  and  $N_{Re}$  continue to rely on  $x$ . Numerical results are deemed appropriate, as long as they yield a locally similarity solution, as emphasized by Habibi and Jahangiri [16]. Additionally,  $M$ ,  $N_F$  and  $N_{Re}$  treated as constants in this context following [16].

### 4. RESULTS AND DISCUSSION

The computed numerical values of  $-\theta'(0)$  in the standard fluid scenario are cross-referenced with Kuznetsov and Nield's findings [3] to validate the accuracy of the calculations. Table 1 illustrates a significant alignment between the two sets of data.

**Table 1.** Comparison of  $-\theta'(0)$

$Pr$	1.0	10.0	100.0	1000.0
$-\theta'(0)$ (Kuznetsov and Nield [3])	0.401	0.463	0.481	0.484
$-\theta'(0)$ (present results)	0.401	0.463	0.480	0.482

Fig. 2 illustrates the distributions of dimensionless longitudinal velocity  $\frac{df(\eta)}{d\eta}$ , concentration  $s(\eta)$  and temperature  $\theta(\eta)$  of the flow.

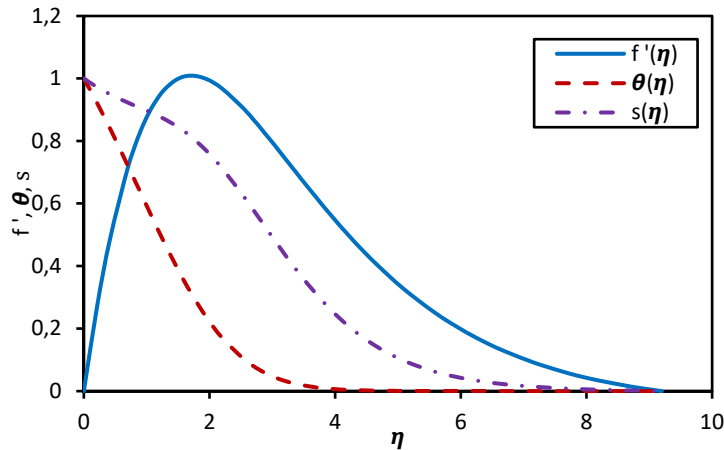


**Figure 2.** Plots of  $\frac{df(\eta)}{d\eta}$ ,  $\theta(\eta)$  and  $s(\eta)$  for the case  $Pr = 6.2$ ,  $N_{Re} = Sc = 2.0$ ,  $Nc = N_F = M = Nr = Nb = Nt = 0.1$ .

#### 4.1. Impact of Electrification Parameter on Velocity, Temperature and Concentration Profiles

Numerical analysis is conducted to investigate the impact of  $M$  on  $f'(\eta)$ ,  $\theta(\eta)$ , and  $s(\eta)$  distributions with respect to  $\eta$ , represented graphically. Figure 3 illustrates the effect of  $M$  on  $f'(\eta)$ , revealing an enhancement in  $f'(\eta)$  with increasing  $M$ .

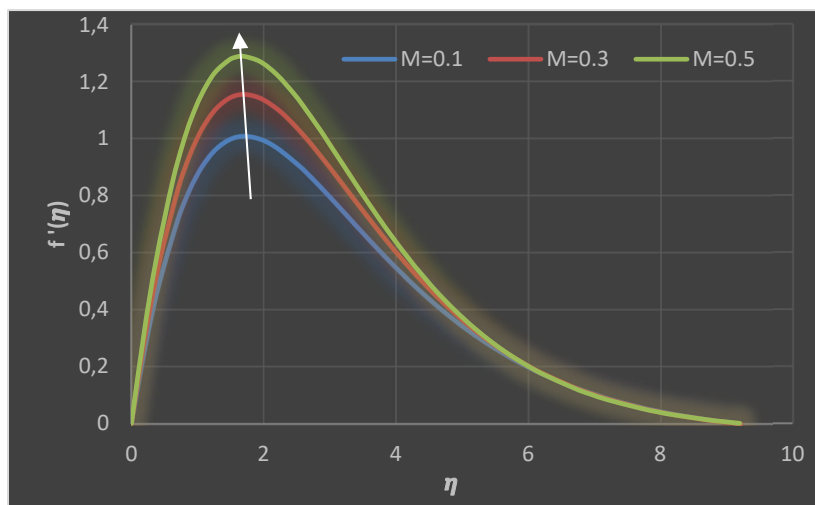


**Figure 3.** Effects of  $M$  on velocity profiles

This phenomenon occurs due to the escalation of the electrification parameter, which subsequently augments the drag force on ions, inducing an opposite and equal reaction force on neutral fluid molecules within the boundary layer,

thereby causing an increase in  $f'(\eta)$ . By increasing  $M$ ,  $\theta(\eta)$  decrease, as shown in Fig. 4. The rise in  $M$  leads to an increase in fluid velocity, causing the hotter fluid particles to move away. Consequently, the fluid cools, resulting in a decrease in  $\theta(\eta)$ . Fig. 5 shows that  $s(\eta)$  reduces with increasing  $M$ . This occurs due to a rise in  $M$ , causing nanoparticles to move from the fluid region towards the flat surface, resulting in a decrease in  $s(\eta)$ . The values  $Pr = 6.2, Nc = N_F = Nr = Nb = Nt = 0.1$  and  $N_{Re} = Sc = 2.0$  remain constant across all the findings depicted in figures 3 to 5.

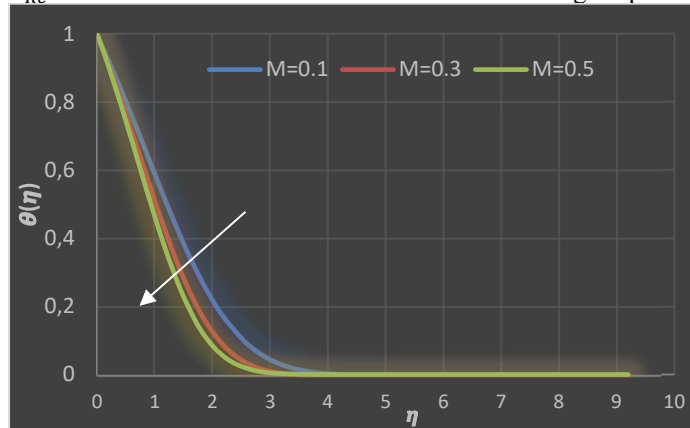


Figure 4. Effects of  $M$  on temperature profiles.

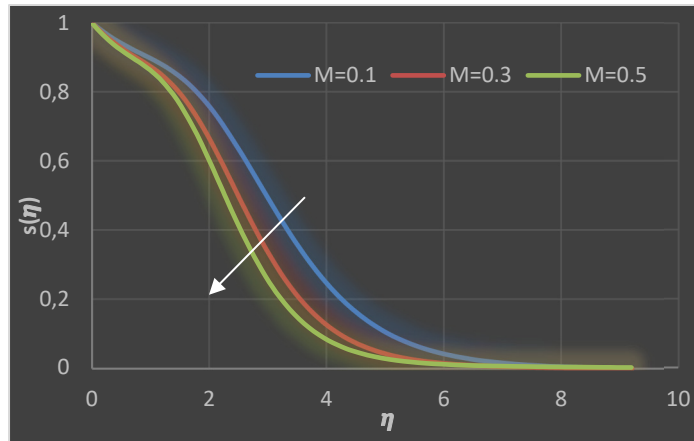


Figure 5. Effects of  $M$  on concentration profiles

#### 4.2. Impact of Electric Reynolds Number on Velocity, Temperature and Concentration Profiles

Numerical investigation is conducted to examine the impact of  $N_{Re}$  on  $f'(\eta)$ ,  $\theta(\eta)$ , and  $s(\eta)$  distributions with respect to  $\eta$ , represented graphically. Figure 6 and 7 shows the effect of  $N_{Re}$  on  $f'(\eta)$  and  $\theta(\eta)$  respectively, revealing an improvement in  $f'(\eta)$  and  $\theta(\eta)$  as  $N_{Re}$  increases. Fig. 8 indicates that  $s(\eta)$  reduces near the flat surface while the opposite trend is noticed far away from the flat surface with increasing  $N_{Re}$ . The values  $Pr = 6.2, Nc = M = N_F = Nr = Nb = Nt = 0.1$  and  $Sc = 2.0$  remain constant across all the findings depicted in figures 6 to 8.

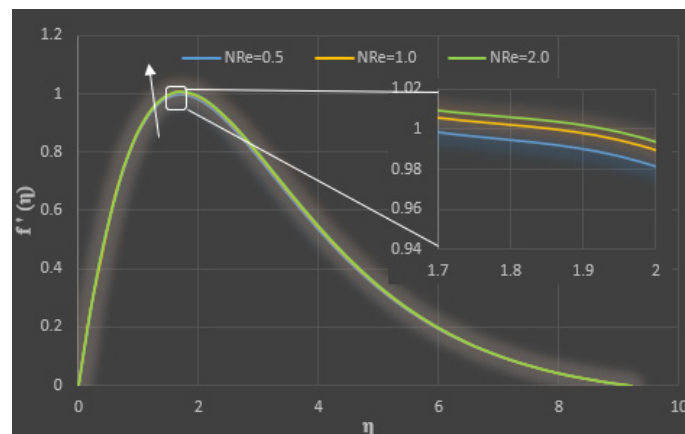


Figure 6. Effects of  $N_{Re}$  on velocity profiles.

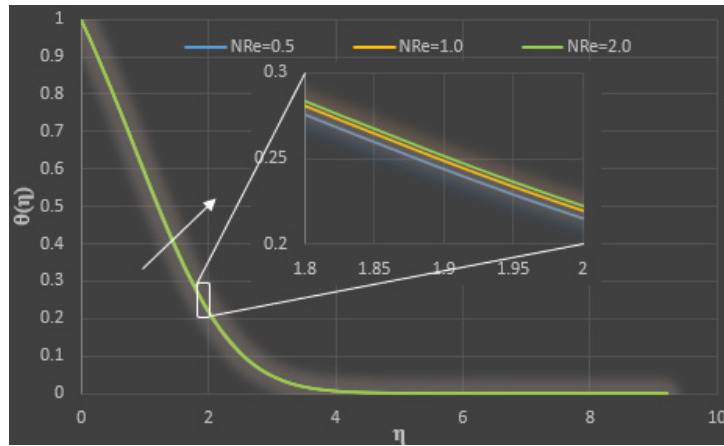


Figure 7. Effects of  $N_{Re}$  on temperature profiles.

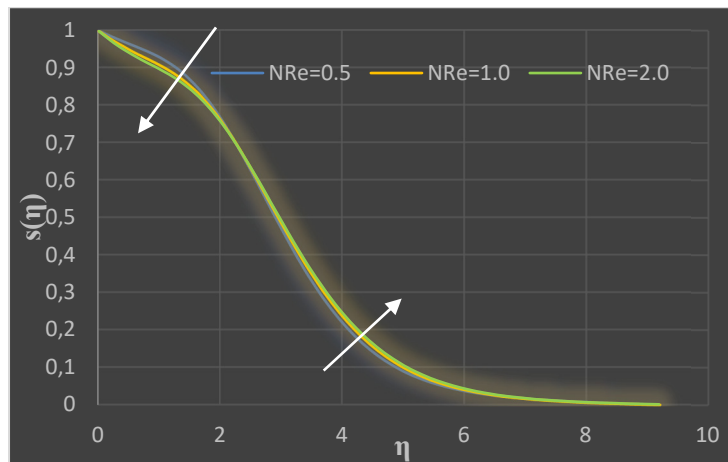


Figure 8. Effects of  $N_{Re}$  on concentration profiles.

#### 4.3. Combined effects of Electric Reynolds Number and Electrification parameter on Non-dimensional Heat and Mass Transfer Coefficients

The combined effects of  $N_{Re}$  and  $M$  on  $-\theta'(0)$  and  $-s'(0)$  is depicted in Table 2. It is observed that for various values of the electric Reynolds number, both  $-\theta'(0)$  and  $-s'(0)$  enhances as  $M$  increases. It has been noted that as the electric Reynolds number ( $N_{Re}$ ) increases,  $-\theta'(0)$  reduces whereas  $-s'(0)$  improves across different values of electrification parameter.

Furthermore, the effect of  $M$  on  $-\theta'(0)$  and  $-s'(0)$  for varied values of  $Nb$  is depicted in Figs. 9 and 10, respectively. It is found that for various values of the Brownian motion parameter, both  $-\theta'(0)$  and  $-s'(0)$  improve as  $M$  grows. This is because as  $M$  grows, the values of  $\theta(\eta)$  and  $s(\eta)$  near the flat surface both drops.

Table 2. Combined effects of  $N_{Re}$  and  $M$  on  $-\theta'(0)$  and  $-s'(0)$  when  $Sc = 2.0, Pr = 6.2, Nr = Nc = Nb = Nt = N_F = 0.1$ .

$M$	$N_{Re}$	$-\theta'(0)$	$-s'(0)$
0.1	0.5	0.37543	0.07865
	1.0	0.36667	0.11995
	1.5	0.36378	0.13370
	2.0	0.36235	0.14057
	2.5	0.36148	0.14469
0.2	0.5	0.41083	0.10685
	1.0	0.40229	0.14506
	1.5	0.39948	0.15774
	2.0	0.39808	0.16407
	2.5	0.39725	0.16786
0.3	0.5	0.43878	0.12520
	1.0	0.43040	0.16132
	1.5	0.42764	0.17330
	2.0	0.42627	0.17926
	2.5	0.42545	0.18284

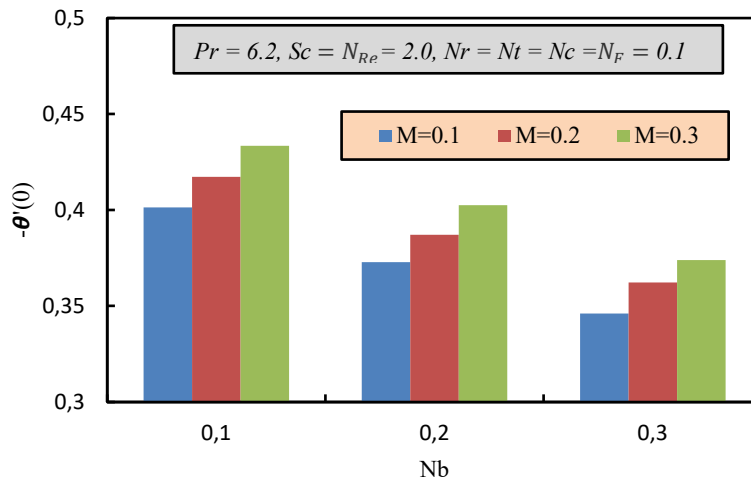


Figure 9. Effects of  $M$  on  $-\theta'(0)$  for varied values of  $Nb$ .

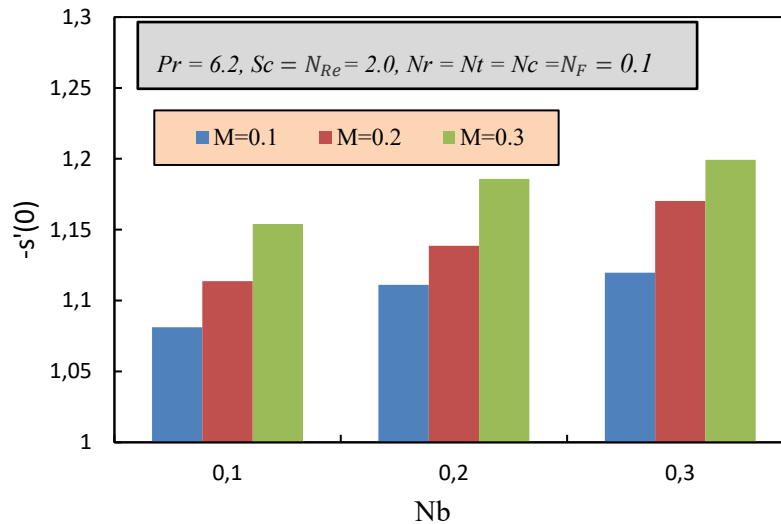


Figure 10. Effects of  $M$  on  $-s'(0)$  for varied values of  $Nb$ .

### 5. CONCLUSIONS

The heat and mass transfer aspects of natural convective nanofluid flow involves examining the impact of  $M$  and  $N_{Re}$  on  $f'(\eta)$ ,  $\theta(\eta)$ ,  $s(\eta)$ ,  $-\theta'(0)$  and  $-s'(0)$ . The numerical investigation focuses on studying the variations of  $-\theta'(0)$  and  $-s'(0)$  concerning the values of  $M$  and  $N_{Re}$ , with the results presented in graphical and tabular forms. The analysis of these findings yields the following conclusions:

- As the electrification parameter  $M$  increases, there is an increase in the non-dimensional velocity, accompanied by a reduction in the dimensionless concentration and temperature within the boundary layer region.
- As the electric Reynolds number  $N_{Re}$  rises, the non-dimensional velocity and temperature experiences a growth, while the dimensionless concentration experiences dual nature within the boundary layer region.
- As the dimensionless heat transfer rate rises from a flat wall to a nanofluid, there's a consequent increase in  $M$ , prompting heat conduction into the cooler fluid and subsequently cooling the flat surface.
- An increase in the values of  $M$  results in a boost in the dimensionless mass transfer rate from a flat surface to a nanofluid, consequently bolstering drug delivery efficacy in biomedical uses.
- The dimensionless heat transfer coefficient decreases as the electric Reynolds number increases.
- The dimensionless mass transfer coefficient enhances as the values of  $N_{Re}$  increase.

Furthermore, alongside thermophoresis and Brownian motion, as proposed by Buongiorno, the inclusion of electrified nanoparticles emerges as a pivotal element in the modelling of nanofluid flow. This aspect notably enhances both heat and mass transfer mechanisms.

### ORCID

## REFERENCES

- [1] S.U.S. Choi, Z.G. Zhang, W. Yu, F.E. Lockwood, and E.A. Grulke, "Anomalous thermal conductivity enhancement in nanotube suspensions," *Applied Physics Letters*, **79**, 2252-2254 (2001). <https://doi.org/10.1063/1.1408272>
- [2] J. Buongiorno, "Convective transport in nanofluids," *ASME J. Heat Transf.* **128**, 240-250 (2006). <https://doi.org/10.1115/1.2150834>
- [3] A.V. Kuznetsov, and D.A. Nield, "Natural convective boundary-layer flow of a nanofluid past a vertical plate," *Int. J. Thermal Sci.* **49**, 243-247 (2010). <https://doi.org/10.1016/j.ijthermalsci.2009.07.015>
- [4] W.A. Khan, and A. Aziz, "Natural convection flow of a nanofluid over a vertical plate with uniform surface heat flux," *Int. J. Therm. Sci.* **50**, 1207-1214 (2011). <https://doi.org/10.1016/j.ijthermalsci.2011.02.015>
- [5] A. Aziz, and W.A. Khan, "Natural convective boundary layer flow of a nanofluid past a convectively heated vertical plate," *International Journal of Thermal Sciences*, **52**, 83-90 (2012). <https://doi.org/10.1016/j.ijthermalsci.2011.10.001>
- [6] S. Das, and R.N. Jana, "Natural convective magneto-nanofluid flow and radiative heat transfer past a moving vertical plate," *Alexandria Engineering Journal*, **54**, 55-64 (2015). <https://doi.org/10.1016/j.aej.2015.01.001>
- [7] M. Goyal, and R. Bhargava, "Simulation of natural convective boundary layer flow of a nanofluid past a convectively heated inclined plate in the presence of magnetic field," *Int. J. Appl. Comput. Math.* **4**, 63 (2018). <https://doi.org/10.1007/s40819-018-0483-0>
- [8] S.P. Jeevandar, V. Kedla, N. Gullapalli, and S.K. Thavada, "Natural Convective Effects on MHD Boundary Layer Nanofluid Flow over an Exponentially Accelerating Vertical Plate," *Biointerface Research in Applied Chemistry*, **11**(6), 13790-13805 (2021). <https://doi.org/10.33263/BRIAC116.1379013805>
- [9] Y.D. Reddy, and B.S. Goud, "Comprehensive analysis of thermal radiation impact on an unsteady MHD nanofluid flow across an infinite vertical flat plate with ramped temperature with heat consumption," *Results in Engineering*, **17**, 100796 (2023). <https://doi.org/10.1016/j.rineng.2022.100796>
- [10] S. Dey, S. Mukhopadhyay, and K. Vajravelu, "Nonlinear natural convective nanofluid flow past a vertical plate," *Numerical Heat Transfer, Part A: Applications*, 1-23 (2024). <https://doi.org/10.1080/10407782.2024.2302966>
- [11] S.L. Soo, "Effect of electrification on the dynamics of a particulate system," *Industrial and Engineering Chemistry Fundamentals* **3**, 75-80 (1964). <https://doi.org/10.1021/i160009a013>
- [12] Z. Kang, and L. Wang, "Effect of thermal-electric cross coupling on heat transport in nanofluids," *Energies*, **10**(1), 1-13 (2017). <https://doi.org/10.3390/en10010123>
- [13] A.K. Pati, A. Misra, and S.K. Mishra, "Effect of electrification of nanoparticles on heat and mass transfer in boundary layer flow of a copper water nanofluid over a stretching cylinder with viscous dissipation," *JP journal of heat and mass transfer*, **17**(1), 97-117 (2019). <http://dx.doi.org/10.17654/HM017010097>
- [14] M. Mahrukh, A. Kumar, S. Gu, S. Kamnis, and E. Gozali, "Modeling the Effects of Concentration of Solid Nanoparticles in Liquid Feedstock Injection on High-Velocity Suspension Flame Spray Process," *Ind. Eng. Chem. Res.* **55**, 2556-2573 (2016). <https://doi.org/10.1021/acs.iecr.5b03956>
- [15] H.F. Oztop, and E. Abu-Nada, "Numerical study of natural convection in partially heated rectangular enclosures filled with nanofluids," *International Journal of Heat Fluid Flow*, **29**, 1326-1336 (2008). <https://doi.org/10.1016/j.ijheatfluidflow.2008.04.009>
- [16] M.H. Habibi, and P. Jahangiri, "Forced convection boundary layer magnetohydrodynamic flow of nanofluid over a permeable stretching plate with viscous dissipation," *Thermal Science*, **18**(Suppl. 2), 587-598 (2014). <https://doi.org/10.2298/TSCI120403049H>

**АСПЕКТИ ПЕРЕНЕСЕННЯ ТЕПЛА ТА МАСИ ПОТОКОМ НАНОФЛЮІДІВ ДО ВЕРТИКАЛЬНОЇ ПЛОСКОЇ ПОВЕРХНІ ПІД ВПЛИВОМ ЕЛЕКТРИФІКОВАНИХ НАНОЧАСТИНОК ТА ЕЛЕКТРИЧНОГО ЧИСЛА РЕЙНОЛЬДСА**

**Адітя Кумар Паті, Суджит Мішра, Ашок Місра, Сародж Кумар Мішра**

*Університет технології та менеджменту Центуріон, Паралахемунді, Одіша, Індія*

У цьому дослідженні розглядаються аспекти тепло- та масообміну природного конвективного потоку нанофлюїду вздовж вертикальної плоскої поверхні, що включає електрифіковані наночастинки та електричне число Рейнольдса. У той час як звичайні моделі нанофлюїдів, такі як модель Буонджорно, не помічають механізми електризації наночастинок і електричних чисел Рейнольдса, це дослідження розглядає механізми електризації наночастинок і електричних чисел Рейнольдса, обґрунтовуючи їх актуальність, особливо коли трибоелектризація є результатом броунівського руху. Таке включення електричного числа Рейнольдса та механізму електризації наночастинок є унікальним аспектом цього дослідження. Використовуючи метод подібності та безрозмірність, керівні диференціальні рівняння в частинних похідних потоку перетворюються на набір локально подібних рівнянь. Розв'язувач `bvp4c` MATLAB використовується для вирішення цього набору рівнянь разом із граничними умовами. Отримані результати підтверджуються порівнянням з результатами раніше опублікованих робіт. Наведено графічні представлення числових результатів безвимірної швидкості, концентрації та температури щодо параметра електризації наночастинок та електричного числа Рейнольдса. У табличній формі розглянуто сукупний вплив параметра електризації наночастинок та електричного числа Рейнольдса на безрозмірні коефіцієнти тепло- та масовіддачі. Крім того, графічно досліджено вплив параметра електризації наночастинок як на тепло-, так і на масообмін для різних значень параметра броунівського руху. Основний висновок цього дослідження вказує на те, що механізм електризації наночастинок прискорює передачу тепла та маси від плоскої поверхні до нанорідини, що передбачає багатообіцяючі перспективи використання в системах охолодження та біомедичних додатках.

**Ключові слова:** *наелектризовані наночастинки; нанофлюїд; модель Буонджорно; електричне число Рейнольдса; природна конвекція*